Lipid Environments in the Yolk Lipoprotein System. A Spin-Labeling Study of the Lipovitellin/Phosvitin Complex from *Xenopus laevis*†

G. Bruce Birrell, Philip B. Anderson, Patricia C. Jost,* O. Hayes Griffith, Leonard J. Banaszak, and Joachim Seelig

ABSTRACT: Lipid/protein and lipid/lipid interactions in the yolk lipoprotein complex from *Xenopus laevis* were examined by introducing a series of lipid spin-labels into the complex and observing the electron spin resonance spectra as a function of the position of the label along the lipid chains, temperature, pH, and charge on the lipid polar head group. Analyses of the spectra show that, in addition to the expected component arising from lipid associated with protein, a second component with increased segmental flexibility and the greater temperature dependence characteristic of lipid/lipid interactions is observed. These spin-labeling data and supporting compositional data indicate that much of the lipid is organized into a lipid-rich region or pool, consistent with the earlier model derived from electron microscopy and diffraction data and with companion ^{31}P and ^{2}H nuclear magnetic resonance data reported in the preceding paper [Banaszak, L. J., & Seelig, J. (1982) *Biochemistry* (preceding paper in this issue)]. The bilayer-like component exhibits a greater restriction of motion compared to vesicles of the isolated lipids at the same temperature, as would be expected for a relatively small lipid pool. Phospholipids exchange between the two motionally distinguishable environments. The equilibrium binding undergoes a shift between these two environments as a function both of pH and of the charge on the phospholipid polar head group. This shift in average binding affinity is opposite in direction to that reported for membrane proteins and implicates negatively charged groups on the protein that repel negatively charged phospholipids. This effect is greatly reduced by alkaline phosphatase treatment, suggesting that some of the lipid binding sites are in close proximity to phosphorylated residues on the protein.

The yolk system of *Xenopus laevis* is one of the small number of lipid and protein systems that have been obtained in a crystalline form (Honjin & Nakamura, 1967). Others include the purple membrane patches from *Halobacterium halobium* (Blaurock & Stoeckenius, 1971; Henderson & Unwin, 1975), the chlorophyll-binding protein of *Chlorobium limicola* (Fenna et al., 1974), special preparations of cytochrome *c* oxidase from the inner mitochondrial membrane (Vanderkooi et al., 1972; Henderson et al., 1977; Fuller et al., 1979), and acetylcholine receptor rich membrane fragments of *Torpedo marmorata* (Ross et al., 1977). Diffraction techniques combined with electron microscopy and image reconstruction are providing details of the three-dimensional structures of these proteins at various levels of resolution. Obtaining information about the organization and dynamics of the lipid components of these systems has proven to be more difficult. Not only is higher resolution required to visualize the lipid than to obtain the general shape of the protein but also the presence of molecular motion of the lipids in the system may affect the diffraction patterns and reduce the effective resolution. The structural organization of the lipid chains has been resolved only in the case of the chlorophyll-binding protein where the phytol chains of chlorophyll are rigidly held (Matthews, 1982). Spectroscopic techniques, such as magnetic resonance, that are sensitive to the time scale of lipid motions, can be used to characterize the lipid organization.

To approach this problem of lipid organization and dynamics in the lipovitellin/phosvitin complex, a collaborative effort between laboratories was initiated so that samples from virtually the same preparations used for the earlier structural studies could be examined by several magnetic resonance techniques. In the previous paper, the results of the nuclear magnetic resonance (NMR)[1] experiments were presented (Banaszak & Seelig, 1982). The purpose of the present paper is to report the electron spin resonance (ESR) data obtained with lipid spin-labels diffused into the lipovitellin/phosvitin complex. In addition, the combined NMR and ESR results are discussed in light of the 20-Å resolution structural model arrived at previously from electron microscopy and diffraction methods (Ohlendorf et al., 1975, 1978). The magnetic resonance experiments are consistent with the model and provide new information about the microscopic environments and particularly the dynamics of the lipids contained in this unusual water-soluble lipoprotein complex.

Materials and Methods

The yolk lipoprotein complex from *Xenopus laevis* was isolated by using the procedure of Ohlendorf et al. (1977). The resulting pale green microcrystals were lyophilized and stored at −20 °C until used. Doxyl spin-labels were synthesized as described by Keana (1979). The lipid spin-labels containing the proxyl moiety at the 14 position were also prepared as previously described (Keana, 1979; Keana et al., 1982), and the structures are shown in Figure 1.

Spin-Labeling Procedures. The yolk complex was labeled with single tail lipid spin-labels by evaporating the solvent from 8 μL of lipid spin-label (1 mg/mL in ethanol) under a stream of dry nitrogen followed by aspiration to remove any traces of organic solvent. The yolk complex (5 mg) was dissolved

† From the Institute of Molecular Biology and Department of Chemistry, University of Oregon, Eugene, Oregon 97403 (G.B.B., P.B.A., P.C.J., and O.H.G.), the Department of Biochemistry, Division of Biology and Biomedical Sciences, Washington University, St. Louis, Missouri 63110 (L.J.B.), and the Department of Biophysical Chemistry, Biozentrum, University of Basel, Basel, Switzerland (J.S.). *Received October 19, 1981.* This work was supported by National Institutes of Health Grants GM 25698 and GM 13925 and by Swiss National Science Foundation Grant 3.746.80. L.J.B. is grateful to the Josiah Macy Foundation, New York, and the Roche Foundation, Basel, for their financial help during this period.

[1] Abbreviations: NMR, nuclear magnetic resonance; ESR, electron spin resonance; BSA, bovine serum albumin; LV/PV, lipovitellin/phosvitin complex; doxyl, 2,2-disubstituted 4,4-dimethyloxazolidinyl-*N*-oxy; proxyl, 2,2-disubstituted 5,5-dimethylpyrrolidinyl-*N*-oxy; PC*, PG*, QA*, and MP*, lipid label structures shown in Figure 1 (the asterisk indicates that the molecule carries the spin-label moiety); EDTA, ethylenediaminetetraacetic acid.

0006-2960/82/0421-2444$01.25/0

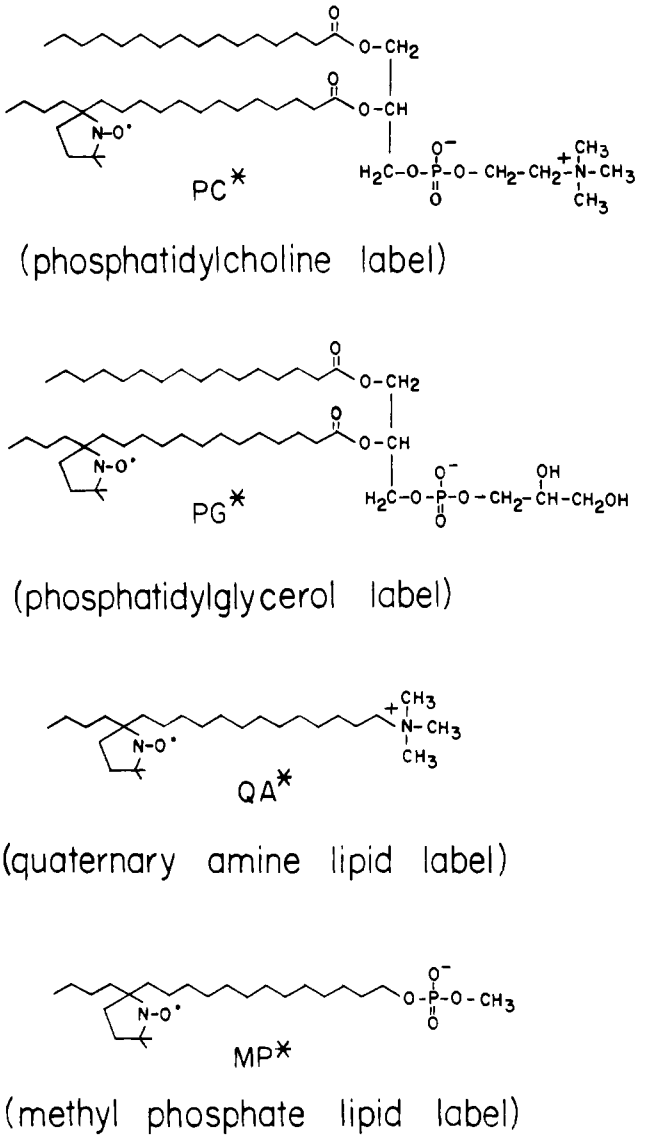

FIGURE 1: Structures of the 14-proxyl lipid spin-labels used in this study. The abbreviations are starred to indicate that the lipid is a spin-label.

in 250 μL of 0.2 M phosphate, 0.5 M NaCl, and 1 mM EDTA buffer of either pH 5.5 or 7.8. The same buffer was used in all experiments unless otherwise specified. The pH was routinely rechecked, after addition of the protein, since the large number of phosphate groups present on the polypeptides of the complex can alter the pH of the buffer at pH 5.5 and 7.8 if the buffer capacity is too low. The solubilized complex in 200 μL was added to the vial containing the spin-label and mixed by low power bath sonication at 0 °C for ~5 min. Alternatively, incorporation of the lipid spin-labels in the yolk complex was achieved by incubation of dry spin-label and complex at room temperature for 20 min with occasional swirling. ESR spectra of the spin-labeled complex obtained with either procedure were essentially the same. Protein concentration was accomplished by centrifugation at 100000 rpm (160000*g*) with a Beckman airfuge operated at room temperature, yielding a clear gelatinous lower phase. The concentration step was carried out to reduce the noise level in the ESR spectra. ESR line shapes were not affected by concentration of the sample. Labeling of the microcrystals followed the same procedure, but with 0.5 M NaCl omitted from the buffer. In either case, ~15 μL of buffer was added to the concentrated protein (lower phase) and transferred to a melting point capillary, which was then inserted in a quartz ESR tube for ESR measurement.

Phospholipid spin-labels were incorporated in the yolk complex by ethanolic injection. The complex (12 mg) was first dissolved in 250 μL of buffer, and 5 μL of a stock solution of spin-label (5 mg/mL) in ethanol was added to the dissolved yolk complex over a period of 20 min with stirring. The solution was incubated at room temperature for 12 h, and then 175 μL was removed and centrifuged at 100000 rpm in a Beckman airfuge. ESR spectra were recorded on the gelatinous lower phase. As a control, 5 μL of ethanol was slowly added to 250 μL of buffer containing 12 mg of complex previously labeled with the single tail lipid spin-label QA*. ESR spectra of the spin-labeled complex obtained before and after ethanol addition were identical, indicating that the small amount of ethanol was not affecting the experimental results.

The total lipid extract from the yolk complex was obtained by using the method of Bligh & Dyer (1959). For spin-labeling, PC* in benzene was added to the lipids (containing ~30 mg of phospholipid) dissolved in chloroform at a mole ratio of spin-label to lipid of 1 to 150. After the bulk of the solvent was evaporated under a stream of dry nitrogen, the last traces were removed in a trapped vacuum system. The mixture was then resuspended in 1 mL of buffer (pH 7.8) by bath sonication.

For spin-labeling of bovine serum albumin, 25 mg of BSA (Pentex fatty acid poor) was first dissolved in pH 7.8 buffer, added to a vial containing a dry film of 32 μg of 14-proxyl-stearic acid, and bath sonicated at 0 °C for 10 min.

Protein Modification. The yolk complex was treated with alkaline phosphatase by using essentially the procedure of Burley & Cook (1962). The complex (20 mg) was first dissolved in 1 mL of 0.3 M sodium bicarbonate, pH 8.1. A 30-μL aliquot of a solution of alkaline phosphatase (Sigma, type III from *Escherichia coli*) in 2.5 M $(NH_4)_2SO_4$ containing 18 mg of protein/mL (22 units/mg of protein) was added. The mixture was stirred, placed in a dialysis bag (Spectrapor 2), and dialyzed against 0.3 M sodium bicarbonate, pH 8.1, at 37 °C.

The phosphatase-treated complex and the lipids extracted from the phosphatase-treated complex were analyzed for inorganic phosphorus by the procedure of Lowry & Tinsley (1974). Protein content was estimated by using the method of Lowry et al. (1951) as modified by Miller (1959), with BSA as the standard.

Instrumentation. ESR spectra were recorded on a Varian E-line 9.5-GHz ESR spectrometer equipped with field/frequency lock and interfaced to a 32K Varian 620L/100 computer. Treatment of the digitized data is described elsewhere (Brotherus et al., 1980). A microwave power setting of 5 mW was used for all samples, and temperatures were controlled to ±0.2 °C.

Circular dichroism spectra of solutions of the yolk complex (0.5 mg/mL in 0.5 M phosphate and 0.5 M NaCl, pH 5.5 and 7.8) were obtained on a Jasco J-500C spectropolarimeter. CD spectra were obtained over the range 260–200 nm; a cell path length of 0.5 mm was used. No apparent changes in the ellipticity or significant changes in secondary structure of the solubilized complex could be detected as a function of pH in the range from 5.5 to 7.8.

Results

Molecular Motion along the Fatty Acid Chains in the Yolk Lipoprotein Complex. Lipid spin-labels containing the doxyl moiety at various positions along the stearic acid chain were diffused into aqueous solutions of the yolk complex, lipids extracted from the complex, and bovine serum albumin; ESR

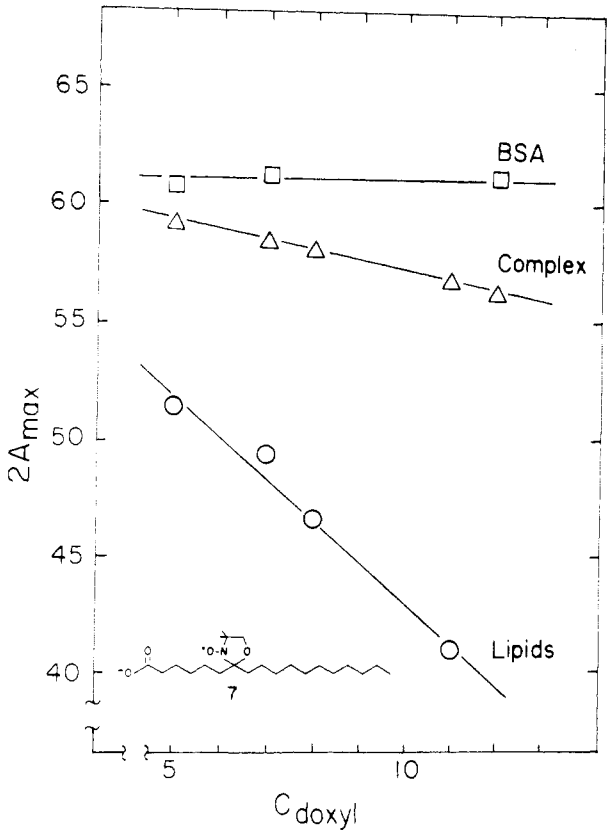

FIGURE 2: Molecular motion along the fatty acid chains of the lipids in the yolk lipovitellin complex. The outermost splitting ($2A_{max}$) is plotted as a function of the position of the nitroxide group on the stearic acid molecule. The carbons are numbered from the carboxyl group, and C_{doxyl} indicates the position of attachment of the nitroxide moiety (inset shows the 7-doxylstearic acid label). For comparison, corresponding measurements on vesicles of lipids extracted from the complex and on bovine serum albumin are also included. All samples were in 10 mM Tris, 0.5 M NaCl, and 0.005% NaN_3 (pH 8.5), and all spectra were recorded at 27.5 °C.

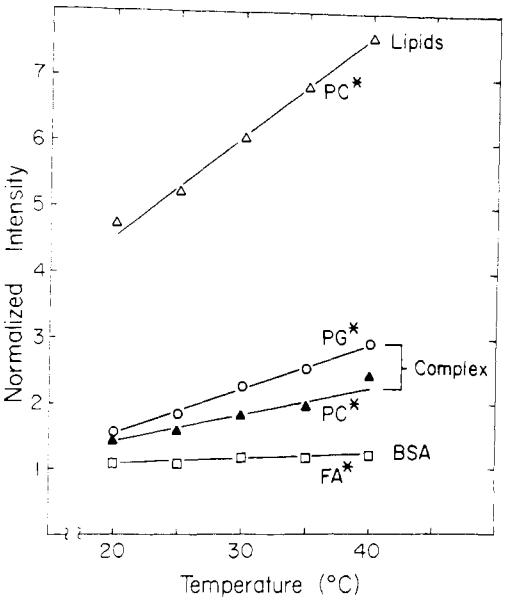

FIGURE 3: Comparison of 14-proxyl lipid labels in the lipovitellin/phosvitin complex, vesicles of lipids extracted from the complex, and bovine serum albumin as a function of temperature. The normalized intensities, i.e., the relative values of the spectral intensities, are obtained by normalizing all spectra to the same arbitrary value for the integrated absorption. The normalized intensity bears an inverse relationship to the line width. From top to bottom, the samples are vesicles of lipids extracted from lipovitellin labeled with PC* (△), yolk lipoprotein complex labeled with PG* (○) and PC* (▲), and bovine serum albumin labeled with 14-proxylstearic acid (□). All samples are buffered at pH 7.8. Note that the steep slope of the top line is characteristic of all of these labels in lipid bilayers. The negligible slope of the bottom line is typical of the relative temperature insensitivity of the line shape of lipid labels immobilized in serum albumin binding sites and is used to illustrate a limiting case where lipids are in individual binding sites surrounded by protein.

spectra were recorded at 27.5 °C. The splittings in gauss between the low-field maximum and high-field minimum ($2A_{max}$) were measured and plotted in Figure 2 as a function of the position of the doxyl group on the stearic acid chain. This parameter has been shown to be sensitive to the motion of the lipid tails (wobble of the doxyl group containing the unpaired electron) and indicates that the amplitude and frequency of the motion increase toward the center of the bilayer (Seelig, 1970; Jost et al., 1971; Hubbell & McConnell, 1971). The variation in $2A_{max}$ with doxyl position in lipids extracted from the yolk complex (Figure 2) is typical of the behavior of this parameter in lipid bilayers. This well-known flexibility profile detected by spin-labeling differs in detail from that obtained by NMR, but nevertheless is characteristic and useful in identifying bilayer-like behavior (McConnell, 1976). In the solubilized complex, the value of $2A_{max}$ is larger and much less dependent on doxyl position, although there is a systematic decrease in this parameter as the doxyl group is moved between the 5 and 12 positions. There is essentially no change in $2A_{max}$ for the reference sample, BSA. This sample was chosen as a limiting case and not intended to represent a model for the yolk lipoprotein system.

Molecular Motion as a Function of Temperature in the Yolk Lipoprotein Complex. For this study, the spin-label (proxyl group) was fixed at the 14 position, near the hydrocarbon terminus, and the temperature was varied. The labels used were phospholipid analogues, except for the fatty acid which binds more efficiently to BSA. ESR spectra of the samples at pH 7.8 were recorded in 5 °C increments between 20 and 40 °C. For comparison, the spectra were first normalized to the same integrated intensity (i.e., to represent the same number of spin-labels and spectrometer gain). Relative center line heights (arbitrary scale) of the normalized spectra are plotted as a function of temperature in Figure 3. The upper curve shows the characteristic behavior of phospholipids (and stearic acid) labeled at the 14 position in lipid bilayers. In the complex, on the other hand, phospholipid spin-labels exhibit only a moderate response to temperature. The motion of the fatty acid in the lipid binding sites of BSA is relatively temperature insensitive.

Some of the individual normalized line shapes that were used to construct Figure 3 are shown in Figure 4. Here it is evident that the line shapes from the complex show more than one spectral component (arrows *a* and *b*). This is especially clear in the 35 °C spectra where the line width of the *a* component is much narrower, although the relative contributions of the two components to the spectral intensity are the same at 20 and 35 °C. Component *a* is a fluid bilayer-like component, and *b* arises from lipid in contact with protein (Jost & Griffith, 1980; Marsh & Watts, 1982). Qualitatively, it is clear that more of component *a* is present when the label is negatively charged and the sample is at pH 7.8. The difference between the PC* and PG* labels seen in Figure 3 and the top row of Figure 4 is essentially abolished by shifting the pH to 5.5. The changes occur in the PG* spectra, while the PC* spectra are independent of pH. The line shape of the spin-labels in extracted lipids (bottom row, Figure 4) represents a single spectral component having a much narrower line width and is essentially pH insensitive. This observation of a single

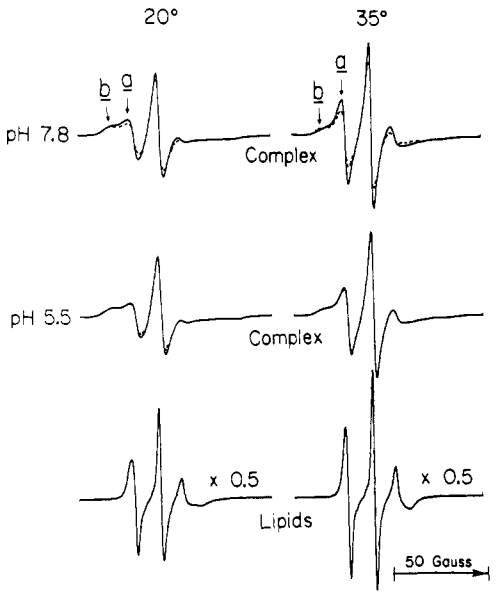

FIGURE 4: Effect of pH on the behavior of a pair of 14-proxyl phospholipid spin-labels (different only in the polar head group) in the yolk lipoprotein complex. In the top two rows, the solid lines are spectra from the complex labeled with PG*, and the dashed lines are for samples labeled with the analogous PC*. The pairs of spectra are superimposed for comparison when only the charge on the phospholipid head group is altered. Spectra of samples at 20 and 35 °C are shown. Spectra in the third row show the general behavior of these labels in vesicles of the extracted lipids, where the data shown are for PC* at pH 7.8. All spectra are normalized to the same integrated absorption except for the spectra in the bottom row which have been scaled down by a factor of 2 to reduce the overall size of the figure.

component in the extracted lipids rules out the possibility that the two spectral components observed in the intact complex could arise from a distribution of labels between the phospholipid phase and a neutral lipid phase with limited phospholipid solubility.

Comparison of Labeled Lipids with Negatively and Positively Charged Polar Head Groups. For further investigation of the difference in lipid binding as a function of polar head-group charge, a pair of single acyl chain spin-labels with opposite charges were diffused into the solubilized yolk complex. The contrast between the behavior of the single tail labels 14-proxyl quaternary amine (QA*, positively charged) and the 14-proxyl monomethyl phosphate (MP*, negatively charged) is shown in Figure 5 (left column). At pH 7.8, the spectrum of the complex containing the negatively charged label (dashed line) has appreciable contributions from both the fluid (*a*) and bound (*b*) components, whereas in the spectrum of the sample containing the positively charged label (solid line) the bound component is much more prominent. At pH 5.5, a third component (*c*) with a larger splitting ($2A_{max}$ = 71–72 G) appears in the spectrum. This very broad component *c* is present only in the spectrum of the complex solubilized in 0.5 M NaCl at the lower pH. Component *c* is not seen when the microcrystals are labeled in low salt at pH 5.5. In the microcrystals, these two labels show a smaller difference at pH 7.8, but the changes with pH are qualitatively similar to the solubilized complex shown in Figure 5. The trend is toward diminishing the spectral difference between the labels in the complex at low pH, as was found for the phospholipid labels (Figure 4).

To determine whether the negatively charged phosphorylated polypeptides are involved in the differences in charge-dependent lipid distribution, we treated the solubilized complex with alkaline phosphatase. The general time course of

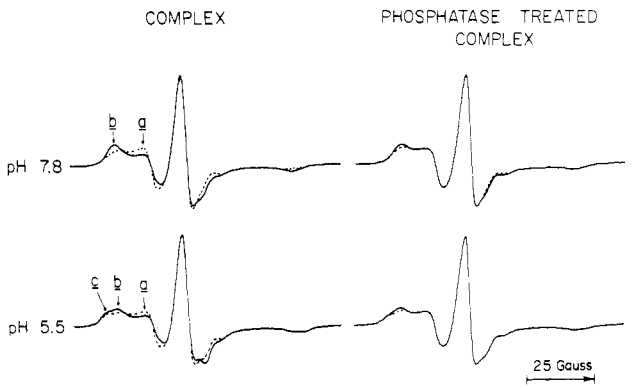

FIGURE 5: Comparison of spectral line shapes before and after treatment of solubilized yolk lipoprotein complex with alkaline phosphatase. Spectra of samples labeled with the positively charged quaternary amine lipid label (solid lines) are superimposed on those labeled with the negatively charged methyl phosphate lipid label (dashed lines). At the higher pH, two separable spectral components *a* and *b* are present. Alkaline phosphatase treatment alters the relative amounts of these two components. At the lower pH (5.5), a third component (*c*) appears in the spectra of the solubilized complex but is removed by the alkaline phosphatase treatment, which reduced the protein and lipid phosphorus contents to 8.9 and 4.9 μg of P_i/mg of protein, respectively. Spectra were recorded at 20 °C and are plotted normalized to the same arbitrary center line height.

Table I: Effect of Phosphatase Treatment on Protein and Lipid Phosphorus Content[a] of the Yolk Complex

time of treatment (days)	total P_i/ protein	lipid P_i/ protein	protein P_i[b]/ protein
0	18.1	5.5	12.6
1	13.5	4.0	9.5
2	11.1	3.5	7.6
3	10.5	3.7	6.8
7	9.1	3.2	5.9

[a] Units of the phosphorus to protein ratios are μg of P_i/mg of protein, estimated errors ±0.2 μg of P_i/mg of protein. The protein reference used is bovine serum albumin which slightly overestimates the protein concentration. The initial (t = 0) protein values are ~10% higher than those of Ohlendorf et al. (1977), who used amino acid analysis to determine the protein concentration. [b] By difference.

phosphate hydrolysis is shown in Table I, although there is considerable variation in the rate of hydrolysis between different runs. Phosphorus is lost from the protein, but it is also lost from the lipids. However, the size of the lipid pool, in terms of the number of acyl chains, is apparently unaffected by moderate phosphatase treatment since control experiments with a neutral label (14-proxyloctadecanol) give identical spectra before and after a phosphatase treatment that removes 30% of the protein phosphorus and 10% of the lipid phosphorus. For the 10% of the phospholipid phosphate that is hydrolyzed, apparently the resulting diglycerides remain in the complex. The essential point is that limited alkaline phosphatase treatment dramatically reduces the difference between the oppositely charged labels as shown in Figure 5. This treatment essentially abolishes the pH effect. In addition, component *c* is no longer resolvable.

The top line of Table I gives a direct chemical analysis of the ratio of protein phosphorus to lipid phosphorus in the intact complex. This ratio is 12.6/5.5 = 2.3, which agrees with the ratio obtained independently by ^{31}P NMR in the preceding paper (Banaszak & Seelig, 1982).

Separation and Quantitation of Spectral Components. The pairwise subtraction method of Brotherus et al. (1980) was used in order to obtain quantitative estimates of the contri-

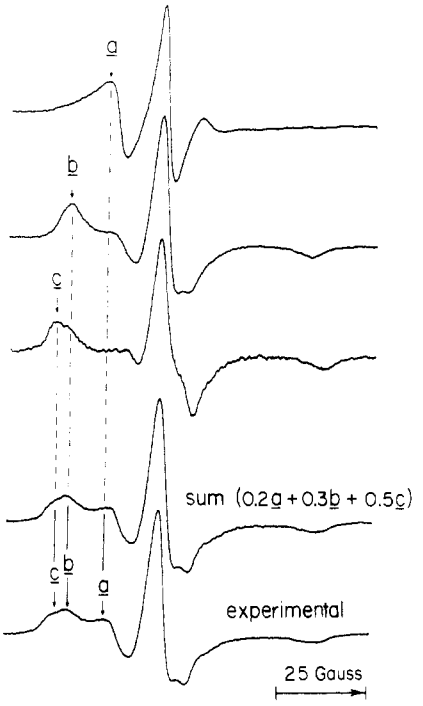

FIGURE 6: Spectral analysis of the pH 5.5 yolk complex spectrum of Figure 5 (solid line, lower left). Appropriate combinations of experimental spectra (20 °C) in Figures 4 and 5 were used in pairwise subtractions (Brotherus et al., 1980) to separate out the basic line shapes, *a*, *b*, and *c*. The experimental spectrum (bottom) is well matched by a simple sum of these line shapes. All spectra are scaled to constant center line height. Fractions contributing to the sum are normalized so that, for example, 0.5*c* indicates 50% of the total absorption is contributed by the *c* component. The unusually large splitting (*c*) is seen only with single chain labels in the solubilized complex at the lower pH.

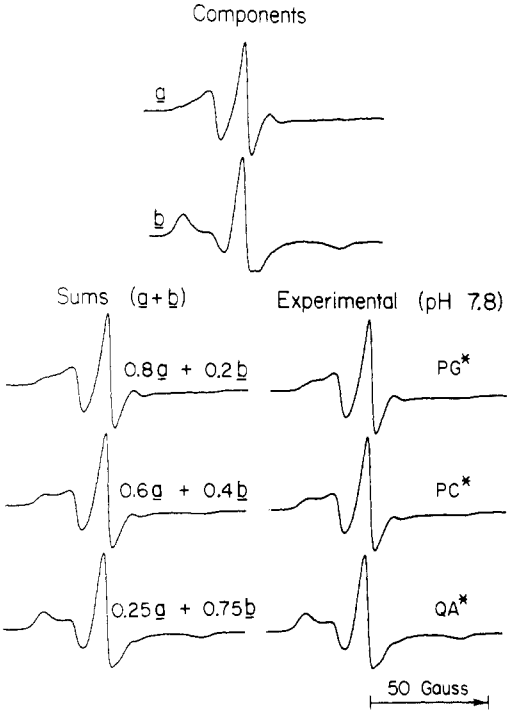

FIGURE 7: Representative spectral analyses involved in determining the relative amounts of lipid in contact with protein (*b*) and lipid exhibiting bilayer-like behavior (*a*) reported in Table II. In this example, relative amounts of spectral components *a* and *b* are summed to match three experimental spectra. Experimental spectra labeled PG* and PC* are the solid and dashed line spectra, respectively, of Figure 4 (upper left), and QA* is the solid line spectrum of Figure 5 (upper left). All spectra are plotted to constant center line height, and fractions refer to the normalized value of the absorption.

butions of the various spectral components in the ESR spectra of Figures 4 and 5. This method makes no assumptions about the line shapes of the components but requires that the pairs of spectra be linear combinations of the same line shapes. Representative line shapes obtained by this procedure are shown in Figure 6. For this example, the top two line shapes, components *a* and *b*, were obtained by using the pair of spectra for PC* and QA* at pH 7.8. The third line shape, component *c*, was obtained by using the pair of spectra from samples labeled with QA* (pH 5.5) before and after phosphatase treatment. Spectral components *a* and *b* are the fundamental line shapes common to all of our experimental spectra. Although there were minor variations in splittings in some cases, these line shapes were reproduced by using many different combinations of spectral pairs obtained during this study.[2] This is also the case for component *c*. The prominent low-field spectral features of these components are indicated in Figure 6 and in the sum arrived at as a match for the experimental spectrum at the bottom of Figure 6. The match between the experimental and summed spectra is excellent. The experimental spectrum is composed of approximately 20% component *a*, 30% component *b*, and 50% component *c*.

Component *c* is observed only with single tail lipid labels at low pH in the solubilized complex and represents an unusual environment in which there is essentially no residual motion on the ESR time scale. Most of the experimental spectra contain only the two components *a* and *b* and can be analyzed by linear combinations of these as shown in Figure 7. Excellent agreement was obtained between the summed spectra and experimental spectra, and the fractions of the two components arrived at by this procedure are presented in Table II.

Table II: Spectral Components Resolved from Composite ESR Line Shapes[a]

preparation	spin-label	pH	fraction fluid (F_a)	fraction bound (F_b)
yolk complex	PC*	7.8	0.60	0.40
yolk complex	PC*	5.5	0.60	0.40
yolk complex	PG*	7.8	0.80	0.20
yolk complex	PG*	5.5	0.65	0.35
yolk complex	QA*	7.8	0.25	0.75
phosphatase-treated yolk complex	QA*	7.8	~0.35	~0.65
yolk complex	MP*	7.8	0.55	0.45
phosphatase-treated yolk complex	MP*	7.8	~0.50	~0.50

[a] Fractions are estimated to be accurate to ±0.03. Fluid refers to spectral component *a* and bound to component *b* in Figures 4–7.

Table II presents an overall picture of the lipid behavior in the yolk complex. The shift in the fractions of the two components with pH is reversible and argues that there is an equilibrium distribution of lipids between the two environments, fluid and bound, giving rise to the components *a* and *b*. The distribution of PC* is a convenient reference since most of the phospholipid present in the yolk complex is phosphatidylcholine. The PC* data indicate that a significant fraction of lipid (60%) is in a bilayer-like environment and this fraction

[2] The outermost splitting for the bound component *b* is in the range normally seen for the similar component in membrane samples. Component *b* is slightly larger (~1 G) for PG* at low pH and MP* at both pHs. The origin of this slight difference in splitting was not further investigated.

remains constant over the pH range investigated. The behavior of the other spin-labels can be viewed as shifts in the equilibrium binding of solute lipids to protein relative to the solvent lipid PC (Brotherus et al., 1981). Shifts are observed as a function of polar head-group charge and of pH.

Discussion

General Characteristics of the ESR Spectra and Comparison with Data from Biological Membranes. Lipids in a fluid bilayer (or monolayer) environment can be distinguished from lipids bound to protein by using spin-labeling. Lipids in a bilayer, where the interaction is dominated by lipid/lipid contacts, exhibit a characteristic flexibility profile. The molecular motion increases along the chain and is greatest at the center of the bilayer, as evidenced by a decrease in the overall splitting $2A_{max}$ of the ESR spectra. There is also a well-known temperature dependence of the ESR spectrum, with the lines becoming much narrower at higher temperatures because of the increased amplitude and frequency of segmental motion of the lipid chains. In contrast, lipid in contact with a membrane protein exhibits very small changes in motion along the hydrocarbon chains (Dehlinger et al., 1974) and a relatively small temperature dependence (Brotherus et al., 1980). Figures 2 and 3 show that the general behavior of the lipid spin-labels in the yolk lipoprotein complex is intermediate between bilayer behavior and the behavior of label bound to the lipid-binding protein, bovine serum albumin. The detailed analysis of the line shapes shows that this arises from a combination of lipid/lipid interactions and lipid/protein interactions.

Analyses of the ESR line shapes show that two components are present in most of the spectra. One component, labeled *b*, is motionally restricted on the ESR time scale. This means that the amplitudes and/or rates of segmental fluctuations are reduced. Component *b* is characteristic of lipid associated with the hydrophobic surfaces of proteins (Jost et al., 1973, 1977; Knowles et al., 1979). The other component, labeled *a*, exhibits a higher degree of molecular motion and a temperature dependence characteristic of lipid/lipid interactions as observed, for example, in lipid bilayers. This more mobile component exhibits somewhat greater restriction of motion than is seen in the isolated lipids at the same temperature. These two lipid domains are reminiscent of membrane data at low lipid:protein ratios, i.e., limited bilayer regions interacting with hydrophobic protein surfaces, as observed in the (Na,K)-ATPase (Brotherus et al., 1980). Component *b* shows restricted motion but is not fully immobilized, unlike the extreme case where each lipid chain is surrounded by protein and held rigidly in a protein matrix. Examples more nearly approaching this more restricted limit are fatty acids bound to BSA (Figure 3) and phospholipids bound to the phospholipid transfer proteins (Devaux et al., 1977; Machida & Ohnishi, 1978).

The ESR spectra are different from those obtained from the quasi-crystalline purple membrane patches of *Halobacterium halobium* where almost all of the lipid (>85–90%) is in contact with protein (Jost et al., 1978). The yolk lipoprotein complex exhibits much more of the bilayer-like component than is seen in the purple membrane.

The striking impression is that these spin-labeling results on the lipovitellin/phosvitin complex closely resemble those of biological membranes known to contain phospholipid bilayers. These data, independent of the NMR data, provide evidence for the presence of limited pools of phospholipid bilayers bounded by hydrophobic protein surfaces of the lipovitellin/phosvitin complex.

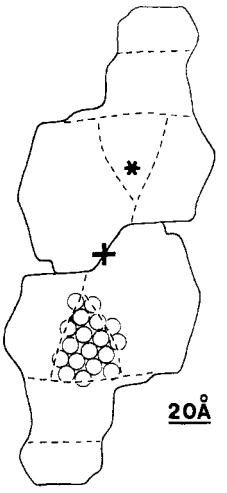

FIGURE 8: Low-resolution model of the lipovitellin complex. The drawing of the complex is similar to the one used to describe the results of electron density matching on the lipovitellin complex (Ross et al., 1980). Two identical subunits of the dimeric molecule are shown with the local symmetry dyad indicated by the cross in the center of the model. In one of the lipovitellin subunits, an asterisk marks the location of a region of low electron density thought to be associated with the lipid domain in lipovitellin (Ross et al., 1980). In the corresponding region of the other subunit, 18 circles are drawn to indicate head-group areas for phospholipid. An area of about 48 Å^2 was used to represent each head group by employing the magnification also shown on the drawing. An approximately equal number of phospholipid molecules would be contained in a bilayer-like structure on the opposing hidden surface of the model.

Compatibility of the Magnetic Resonance Data with the Structural Model Derived Previously from Electron Microscopy and Diffraction Methods. Different magnetic resonance studies (^{31}P and ^{2}H NMR, spin-label ESR) have resulted in spectra consistent with lipid organized in bilayer domains (or monolayer domains). This is in agreement with the 20-Å resolution structure arrived at previously by a combination of electron microscopy and diffraction methods (Ohlendorf et al., 1975, 1977; Ross et al., 1980; Banaszak et al., 1982). At 20-Å resolution, the yolk lipoprotein complex resembles a flattened ellipsoid approximately 55 × 115 × 250 Å and is composed of two subunits related by a 2-fold symmetry axis and has a dimeric molecular weight of approximately 456 000. Each monomer contains several polypeptides, one of which is the highly phosphorylated phosvitin. The other polypeptides (*LV-A*, *LV-B*, and *LV-C*) and the associated lipid are collectively referred to as lipovitellin, hence, the name lipovitellin/phosvitin complex. Associated with the dimeric complex are approximately 100 lipids (74 ± 5% phospholipids and the rest neutral lipids), with phosphatidylcholine as the predominant phospholipid.

A single molecule of the lipoprotein complex is shown schematically in Figure 8. Contrast matching studies reveal a region of low electron density, and it has been suggested that this region near the center of each monomer is due to the relatively low electron density of fatty acyl chains clustered into a single lipid domain. In Figure 8, the tentative position of a lipid domain in one of the subunits of the dimeric lipoprotein is shown by an asterisk. The third dimension (55 Å), not seen in Figure 8, is sufficient to accommodate a lipid bilayer (Ross et al., 1980). The lower part of Figure 8 shows an attempt to fit 18 phospholipid head groups, i.e., one-half of the bilayer, into the available low-density area. The alternative, the presence of nearly 40 phospholipid molecules in a monolayer-like phase, would mean that the surface area covered by the phospholipid head groups would have to be

doubled from that shown in Figure 8. The result would be that much of the surface visible in the drawing would be covered with phospholipid.

The model of Figure 8 is in agreement with the NMR and ESR results, and the presence of lipid domains containing the phospholipid in the form of a bilayer also has attractive thermodynamic aspects to both assembly processes and the stability of the final lipid/protein complex. A microdomain of bilayer lipid in an aqueous environment would only require a limited stabilization factor on its periphery. Such a factor can be provided by the globular protein components *LV-A*, *LV-B*, and *LV-C* present in lipovitellin.

Comparison of the Information on Lipid Environments and Dynamics in the Lipovitellin/Phosvitin Complex Obtained from the ESR and NMR Experiments. The magnetic resonance experiments provide considerably more information than can be shown by a static picture such as Figure 8. It is of interest to compare the NMR and ESR results, since the types of information are different.

The solid-state ^{31}P NMR experiments detect the molecular motion of the phosphate groups, both of the phosphorylated serines and of the phospholipids (Banaszak & Seelig, 1982). The difference in chemical shifts is sufficient to resolve the two classes of phosphates, and with the appropriate choice of pulse and recovery times, it is possible to monitor essentially all of the phospholipids in the complex. From the molecular motion of the head groups (e.g., axially symmetric rotation or lack of it), it is possible to infer the motional behavior of the entire phospholipid molecule. The ^{31}P (and ^{2}H) NMR experiments cover a comparatively slow time scale (10^{-4}–10^{-5} s), which permits the observation of events occurring over a relatively large frequency range.

The spin-labeling experiments, on the other hand, detect the degree of molecular motion of a label attached at various positions along the hydrocarbon chains. What is being measured, therefore, is the motional degree of freedom of lipid chains in environments accessible to the lipid spin-labels. The spin-labels are used in very small concentrations and, in the case of the phospholipid labels, closely resemble natural lipid components of the complex. Because of the short time scale of the ESR experiment (10^{-10}–10^{-8} s), it is possible to obtain information about different lipid environments, such as sites in contact with protein and sites surrounded by lipid, information that is averaged together in the NMR experiments by exchange of lipids between sites.

The following conclusions can be drawn for the lipovitellin/phosvitin (LV/PV) system, bearing these differences of techniques in mind. The ^{31}P NMR spectra establish that all of the phospholipid exchanges rapidly on the NMR time scale (exchange rate $>10^5$ s^{-1}) and essentially all of the phospholipid is in the bilayer pool or in contact with nearby protein. This is well established in this case because of the internal intensity control provided by the ratio of phosphorylated serines to phospholipids observed by ^{31}P NMR and confirmed by biochemical analysis, and because of the good signal/noise ratio in these NMR experiments. The spin-label spectra, on the other hand, reveal two components, which means that the phospholipid exchange rate between the corresponding environments must be slower than 10^8 s^{-1}. The residence time of the exchanging lipid in both the pure lipid phase and the lipid/protein interface is thus bracketed by the time scale of the NMR and EPR experiments and lies between 10^{-5} and 10^{-8} s. Indirect evidence for the exchange of phospholipid spin-labels comes also from the systematic variations of the ESR spectra with changes in pH and spin-label head group. The observed intensity changes are consistent with a multiple binding equilibrium between two distinct environments (see below).

Another aspect of the dynamics of the LV/PV bilayer microdomains is measured by the rotational correlation time, τ_c, of the individual lipids. For the intact LV/PV complex, the correlation time of the phosphate segment from ^{31}P NMR data is $\tau_c \simeq 1$ ns at 24 °C. In liposomes formed from the extracted lipids, the motion is faster and the correlation time shorter by a factor of about 1.6 [see footnote 2 of Banaszak & Seelig (1982)].

A similar result follows from a comparison of the spin-label spectra of liposomes (Figure 4, bottom left spectrum) and LV/PV complex component *a* (Figure 7) with computer-simulated spectra (Polnaszek et al., 1973; Polnaszek & Freed, 1975; Hwang et al., 1975). Even though the theoretical spectra are not a perfect match to the experimental spectra shown here, they clearly indicate that the rotational correlation time τ_c for the motion of PC*, labeled at the 14 position of the hydrocarbon chain, is on the order of a few nanoseconds at 20 °C and is detectably slower (ca. a factor of 2) than that observed for the same spin-label in aqueous dispersions of liposomes of the extracted lipids at the same temperature.[3] Comparison of the second component (component *b*, Figure 7) with the same set of computer simulations indicates that the rotational correlation time $\tau_c \geq 10$ ns. The two components *a* and *b* are resolved in the ESR spectra and are averaged by fast exchange in the NMR spectra. Both the ESR and NMR results indicate that the phospholipids in the limited bilayer pools in lipovitellin are in a dynamic fluidlike state approximating that of pure bilayers above the gel to liquid-crystalline phase transition. The effects are similar to those observed in biological membranes where integral membrane proteins perturb the lipid motion but do not remove the essential fluidlike properties of the lipid bilayer regions (Jost & Griffith, 1980; Seelig & Seelig, 1980). The ESR and NMR data do not distinguish between a monolayer or bilayer region, or give information on possible asymmetry of a lipid pool.

Lipid/Protein Interactions. The short time scale of the ESR experiment resolves much if not all of the lipid in contact with the proteins (component *b*, Figure 7) surrounding the pools of lipid bilayer. The best estimate is provided by the PC* spin-labeling data since the majority of the phospholipid in lipovitellin is phosphatidylcholine. The distribution of the PC*, as judged from the integrated ESR spectral components, is on the order of 40% in contact with the protein and the remaining 60% in contact only with other lipids in the limited bilayer pools. This is in good agreement with the model of Figure 8, which predicts that 50–60% of the phospholipid is in contact with the hydrophobic surfaces of the surrounding proteins. (These and other comparisons necessarily ignore the smaller neutral lipid component, whose organization is un-

[3] These numbers are only approximations. The anisotropic motion of these lipids should be described by a set of dynamic parameters (e.g., rotational diffusion tensor elements $R_\parallel$ and $R_\perp$, which refer to motion parallel and perpendicular, respectively, to the long axis of the lipid) and structural parameters (e.g., amplitudes of motion, order parameters, or orientation distribution functions). In general, it is not appropriate to estimate rotational correlation times by comparing the experimental ESR spectra of lipid spin-labels with spectra simulated for isotropic motion because there is an interplay between the dynamic and structural parameters. However, in lipids for motion distal from the polar head group the order parameter is relatively small (large amplitude motion), and in this regime the estimation of rotational correlation times is not very dependent on the value of the order parameter, so that order-of-magnitude estimations of τ_c can be made from comparison with the spectra simulated for isotropic models.

known.) The lipid spin-label in contact with protein is motion restricted and has the same general appearance as lipid in contact with membrane proteins. For convenience, this component is often referred to as bound or boundary lipid vs. the free bilayer lipid. The motion-restricted component is not rigidly held or immobilized on the protein surface. It represents transient contact of lipids exchanging between bilayer and protein-bound sites.

The proteins influence the equilibrium distribution of lipids in the plane of the bilayer. At pH 7.8, replacing the zwitterionic phosphatidylcholine label with the analogous negatively charged phosphatidylglycerol shifts the equilibrium in favor of the lipid pool; i.e., only 20% of the PG* is at the protein boundary compared with 40% of the PC*. Lowering the pH to 5.5 causes no change in the distribution of PC* but increases the fraction of PG* bound to the protein, so that the behavior of these two labels is now similar. The charges on the polar head groups of PC* and PG* are essentially constant over the pH range of 5.5–7.8. Therefore, the shift in the amount of lipid in contact with the protein indicates that there are ionizable functional groups on the protein that influence the lipid distribution. The direction of the shift in equilibrium indicates that the ionizable groups involved are negatively charged and have a pK in the range of 5.5–7.8. The most likely candidates are carboxyl groups and the phosphate groups present in this unusual protein complex, which is highly phosphorylated (Wallace, 1963).

Our results show that there are negative charges on the protein that tend to repel negatively charged lipids. This leads to the prediction that there would be a corresponding attraction for a positively charged lipid. This is, in fact, observed. When the positively charged quaternary amine spin-label is used at pH 7.8, 75% of the label binds to the protein in contrast to less than 50% for either of the negatively charged lipid labels.

The average equilibrium constant for the exchange between two environments is proportional to the ratio of bound to bilayer components (Griffith & Jost, 1979; Brotherus et al., 1981). These ratios, derived from Table II, for the negatively charged PG* relative to the zwitterionic PC* are ~0.37 (pH 7.8) and ~0.81 (pH 5.5), indicating a partial exclusion of the negatively charged lipid from direct contact with the protein. This result is unexpected since previous studies of the equilibrium distribution of phospholipids between the hydrophobic surfaces and the bilayer in membranes have provided evidence for a limited number of sites with increased average affinity for negatively charged lipids. For example, with (Na,K)-ATPase (Brotherus et al., 1980, 1981), cytochrome oxidase (Griffith & Jost, 1979; Cable & Powell, 1980; Marsh & Watts, 1982), and chromatophores from photosynthetic bacteria (Birrell et al., 1978), negative charges on the lipid head group increase lipid binding to the protein. Since all of the studies use similar spin-labels, the difference in behavior between the membrane systems and the yolk complex cannot be an artifact of the technique.

The decrease in average affinity for negatively charged lipids reported here is the first experimental example of protein repelling negatively charged lipids. The unusual phosphorylation of this protein is involved in the charge-dependent lipid behavior. After removal of some of the protein phosphate groups by alkaline phosphatase, the fraction bound of the negatively charged lipid (MP*) increases and that of the positively charged lipid (QA*) decreases. Thus, some of the phosphoserines (and phosphothreonines) (Ohlendorf et al., 1977) are evidently in close proximity to the lipid head groups and influence the lipid/protein interactions. Thus, it is clear that there is some specificity in lipid/protein interactions and this specificity can vary with the functional groups on the protein that are available for interaction with the lipid head groups.

Acknowledgments

We acknowledge helpful discussions with John F. W. Keana, Douglas Ohlendorf, and John R. Silvius and thank Josie Yu for her help in some of the experiments.

References

Banaszak, L. J., & Seelig, J. (1982) *Biochemistry* (preceding paper in this issue).

Banaszak, L. J., Ross, J. M., & Wrenn, R. F. (1982) in *Lipid Protein Interactions* (Jost, P. C., & Griffith, O. H., Eds.) Vol. I, Chapter 5, Wiley-Interscience, New York.

Birrell, G. B., Sistrom, W. R., & Griffith, O. H. (1978) *Biochemistry 17*, 3768–3773.

Blaurock, A., & Stoeckenius, W. (1971) *Nature (London), New Biol. 233*, 152–155.

Bligh, E. G., & Dyer, W. J. (1959) *Can. J. Biochem. Physiol. 37*, 911–917.

Brotherus, J. R., Jost, P. C., Griffith, O. H., Keana, J. F. W., & Hokin, L. E. (1980) *Proc. Natl. Acad. Sci. U.S.A. 77*, 272–276.

Brotherus, J. R., Griffith, O. H., Brotherus, M. O., Jost, P. C., Silvius, J. R., & Hokin, L. E. (1981) *Biochemistry 20*, 5261–5267.

Burley, R. W., & Cook, W. H. (1962) *Can. J. Biochem. Physiol. 40*, 373–379.

Cable, M. B., & Powell, G. L. (1980) *Biochemistry 19*, 5679–5686.

Dehlinger, P. J., Jost, P. C., & Griffith, O. H. (1974) *Proc. Natl. Acad. Sci. U.S.A. 71*, 2280–2284.

Devaux, P. F., Moonen, P., Bienvenue, A., & Wirtz, K. W. A. (1977) *Proc. Natl. Acad. Sci. U.S.A. 74*, 1807–1810.

Fenna, R. E., Matthews, B. W., Olson, J. M., & Shaw, E. K. (1974) *J. Mol. Biol. 84*, 231–240.

Fuller, S. D., Capaldi, R. A., & Henderson, R. (1979) *J. Mol. Biol. 134*, 305–327.

Griffith, O. H., & Jost, P. C. (1979) in *Cytochrome Oxidase* (Chance, B., King, T. E., Okunuki, K., & Orii, Y., Eds.) pp 207–218, Elsevier/North-Holland Biomedical Press, Amsterdam, The Netherlands.

Henderson, R., & Unwin, P. N. T. (1975) *Nature (London) 257*, 28–32.

Henderson, R., Capaldi, R. A., & Leigh, J. S. (1977) *J. Mol. Biol. 112*, 631–648.

Honjin, R., & Nakamura, T. (1967) *J. Ultrastruct. Res. 20*, 400–409.

Hubbell, W. L., & McConnell, H. M. (1971) *J. Am. Chem. Soc. 93*, 314–326.

Hwang, J. S., Mason, R. P., Hwang, L.-P., & Freed, J. H. (1975) *J. Phys. Chem. 79*, 489–511.

Jost, P. C., & Griffith, O. H. (1980) *Ann. N.Y. Acad. Sci. 348*, 391–407.

Jost, P. C., Libertini, L. J., Hebert, V. C., & Griffith, O. H. (1971) *J. Mol. Biol. 59*, 77–98.

Jost, P. C., Griffith, O. H., Capaldi, R. A., & Vanderkooi, G. (1973) *Proc. Natl. Acad. Sci. U.S.A. 70*, 480–484.

Jost, P. C., Nadakavukaren, K. K., & Griffith, O. H. (1977) *Biochemistry 16*, 3110–3114.

Jost, P. C., McMillen, D. A., Morgan, W. D., & Stoeckenius, W. (1978) in *Light Transducing Membranes: Structure, Function and Evolution* (Deamer, D., Ed.) pp 141–155, Academic Press, New York.

Keana, J. F. W. (1979) in *Spin Labeling* (Berliner, L. J., Ed.) Vol. 2, pp 115–172, Academic Press, New York.
Keana, J. F. W., Boyd, S. A., McMillen, D. A., Bernard, E. M., & Jost, P. C. (1982) *Chem. Phys. Lipids* (in press).
Knowles, P. F., Watts, A., & Marsh, D. (1979) *Biochemistry 18*, 4480–4487.
Lowry, O. H., Rosebrough, N. J., Farr, A. L., & Randall, R. J. (1951) *J. Biol. Chem. 193*, 265–275.
Lowry, R. R., & Tinsley, I. J. (1974) *Lipids 9*, 491–492.
Machida, K., & Ohnishi, S. (1978) *Biochim. Biophys. Acta 507*, 156–164.
Marsh, D., & Watts, A. (1982) in *Lipid-Protein Interactions* (Jost, P. C., & Griffith, O. H., Eds.) Vol. 2, Chapter 2, Wiley-Interscience, New York.
Matthews, B. (1982) in *Lipid-Protein Interactions* (Jost, P. C., & Griffith, O. H., Eds.) Vol. I, Chapter 1, Wiley-Interscience, New York.
McConnell, H. M. (1976) in *Spin Labeling* (Berliner, L. J., Ed.) Vol. 1, pp 525–560, Academic Press, New York.
Miller, G. L. (1959) *Anal. Chem. 31*, 964.
Ohlendorf, D. H., Collins, M. L., Puronen, E. O., Banaszak, L. J., & Harrison, S. C. (1975) *J. Mol. Biol. 99*, 153–165.
Ohlendorf, D. H., Barbarash, G. R., Trout, A., Kent, C., & Banaszak, L. J. (1977) *J. Biol. Chem. 252*, 7992–8001.
Ohlendorf, D. H., Wrenn, R. F., & Banaszak, L. J. (1978) *Nature (London) 272*, 28–32.
Polnaszek, C. F., & Freed, J. H. (1975) *J. Phys. Chem. 79*, 2283–2306.
Polnaszek, C. F., Bruno, G. V., & Freed, J. H. (1973) *J. Chem. Phys. 58*, 3185–3199.
Ross, M. J., Klymkowsky, M. W., Agard, D. A., & Stroud, R. M. (1977) *J. Mol. Biol. 116*, 635–659.
Ross, J., Wrenn, R. F., Ohlendorf, D. H., & Banaszak, L. J. (1980) *Ann. N.Y. Acad. Sci. 348*, 408–418.
Seelig, J. (1970) *J. Am. Chem. Soc. 92*, 3881–3887.
Seelig, J., & Seelig, A. (1980) *Q. Rev. Biophys. 13*, 19–61.
Vanderkooi, G., Senior, A. E., Capaldi, R. A., & Hayashi, H. (1972) *Biochim. Biophys. Acta 274*, 38–48.
Wallace, R. A. (1963) *Biochim. Biophys. Acta 74*, 505–518.

Qualitative and Comparative Nature of Mitochondrial Translation Products in Mammalian Cells†

Narayan K. Bhat, Banavadi G. Niranjan, and Narayan G. Avadhani*

ABSTRACT: A method has been described for the efficient incorporation of [^{35}S]methionine into isolated mitochondrial particles from various mammalian tissues. The method involves the incubation of digitonin-treated mitochondrial particles (mitoplasts) in a low sucrose medium. Electrophoretic analysis of ^{35}S-labeled products on sodium dodecyl sulfate–polyacrylamide gels under reducing conditions shows that mitoplasts from Ehrlich ascites cells, mouse liver, and rat liver synthesize 19–24 polypeptide species including some high molecular weight components in the size range of 1.0×10^5. The polypeptide species synthesized in the mitoplast system resemble the cycloheximide-resistant products synthesized in the intact cells with respect to size distribution and total number, although significant quantitative differences between the two systems are observed. Experiments on pulse–chase analysis of ^{35}S-labeled mitochondrial products and the effects of protease inhibitors on the electrophoretic profiles suggest no significant proteolytic degradation during the incubation or analysis. Further, control experiments with nuclease-treated mitoplasts and use of specific protein synthesis inhibitors show that all of the labeled polypeptides are the intramitochondrial translation products. Extensive comparison between the products synthesized in Ehrlich ascites and mouse and rat liver mitochondria, using one- and two-dimensional gels under denaturing conditions, shows striking variations, suggesting possible heterogeneity.

Since the first demonstration by McLean et al. (1958) that rat liver mt[1] can actively incorporate radioactive amino acids into proteins, there have been numerous studies on the characterization of this unique translation system [for details, see O'Brien (1976) and Buetow & Wood (1978)] as well as the nature of mt translation products (Schatz & Mason, 1974; Avadhani et al., 1975) in various cell types. Many of the early studies on the analysis of translation products indicated that mt from varied unicellular eukaryotes as well as from the animal sources may synthesize about eight polypeptides [see Beattie (1971), Schatz & Mason (1974), Sebald et al. (1968), Ibrahim et al. (1973), Coote & Work (1971), Schatz et al. (1972), Lederman & Attardi (1973), and Lansman & Clayton (1975)] in the size range of 6×10^3–5.5×10^4 daltons. In yeast and *Neurospora* it was also shown that the electrophoretic patterns of polypeptides synthesized in the whole cells

† From the Laboratories of Biochemistry, Department of Animal Biology, School of Veterinary Medicine, University of Pennsylvania, Philadelphia, Pennsylvania 19104. *Received June 17, 1981; revised manuscript received November 24, 1981.* This research was supported in part by grants from the National Science Foundation (PCM-8022646) and the U.S. Public Health Service (GM-25073). These results comprise a portion of the thesis being submitted to the Graduate Group of Biochemistry-Biophysics, University of Pennsylvania, for the degree of Ph.D. by N.K.B.

[1] Abbreviations: mt, mitochondria; $NaDodSO_4$, sodium dodecyl sulfate; LES, Lettre Ehrlich ascites cells; Hepes, *N*-(2-hydroxyethyl)-piperazine-*N*′-2-ethanesulfonic acid; CHX, cycloheximide; CAP, chloramphenicol; BSA, bovine serum albumin; EDTA, ethylenediaminetetraacetic acid; Tris, tris(hydroxymethyl)aminomethane; ATP, adenosine 5′-triphosphate; GTP, guanosine 5′-triphosphate.

0006-2960/82/0421-2452$01.25/0